Surface spin–flop transition in a uniaxial antiferromagnetic Fe/Cr superlattice induced by a magnetic field of arbitrary direction

2007 J. Phys.: Condens. Matter 19 136001

(http://iopscience.iop.org/0953-8984/19/13/136001)

IOP PUBLISHING JOURNAL OF PHYSICS: CONDENSED MATTER

J. Phys.: Condens. Matter **19** (2007) 136001 (15pp) doi:10.1088/0953-8984/19/13/136001

Surface spin–flop transition in a uniaxial antiferromagnetic Fe/Cr superlattice induced by a magnetic field of arbitrary direction

M G Pini[1], A Rettori[2,3], P Betti[2], J S Jiang[4], Y Ji[4], S G E te Velthuis[4], G P Felcher[4] and S D Bader[4]

[1] Istituto dei Sistemi Complessi, CNR, Sezione di Firenze, Via Madonna del Piano, I-50019 Sesto Fiorentino (FI), Italy
[2] Dipartimento di Fisica, Università di Firenze, Via G Sansone 1, I-50019 Sesto Fiorentino (FI), Italy
[3] INFM-CNR National Research Center S3, Via Campi 213/A, I-41100 Modena, Italy
[4] Materials Science Division, Argonne National Laboratory, Argonne, IL 60439, USA

E-mail: mariagloria.pini@isc.cnr.it

Received 28 November 2006, in final form 18 January 2007
Published 12 March 2007
Online at stacks.iop.org/JPhysCM/19/136001

Abstract

We studied the transition between the antiferromagnetic and the surface spin–flop phases of a uniaxial antiferromagnetic $[\mathrm{Fe}(14\ \text{Å})/\mathrm{Cr}(11\ \text{Å})]_{x20}$ superlattice. For external fields applied parallel to the in-plane easy axis, the layer-by-layer configuration, calculated in the framework of a mean-field one-dimensional model, was benchmarked against published polarized neutron reflectivity data. For an in-plane field H applied at an angle $\psi \neq 0°$ to the easy axis, magnetometry shows that the magnetization M vanishes at $H = 0$, then increases slowly with increasing H. At a critical value of H, a finite jump in $M(H)$ is observed for $\psi < 5°$, while a smooth increase of M versus H is found for $\psi > 5°$. A dramatic increase in the full width at half maximum of the magnetic susceptibility is observed for $\psi \geqslant 5°$. The phase diagram obtained from micromagnetic calculations displays a first-order transition to a surface spin–flop phase for low ψ values, while the transition becomes continuous for ψ greater than a critical angle, $\psi_{\max} \approx 4.75°$. This is in fair agreement with the experimentally observed results.

(Some figures in this article are in colour only in the electronic version)

1. Introduction

It is well known that when a magnetic field applied along the easy axis of a uniaxial antiferromagnet exceeds a critical value $H_{\mathrm{BSF}} = \sqrt{2H_{\mathrm{E}}H_{\mathrm{A}} + H_{\mathrm{A}}^2}$, where H_{E} is the exchange

field and H_A is the anisotropy field, the system undergoes a first-order phase transition to a bulk spin–flop (BSF) phase, characterized by sublattice magnetizations nearly perpendicular to the field direction [1, 2]. In the case of a uniaxial antiferromagnet with one or two surfaces, which break the translational invariance in the direction perpendicular to the surface plane, the problem of determining the ground-state spin configuration in the presence of an external magnetic field applied along the in-plane easy axis was theoretically posed a few decades ago. The first model to be investigated was that of a semi-infinite stack of ferromagnetic planes, antiferromagnetically coupled and subject to a magnetic field antiparallel to the magnetization of the surface plane. For this system, when the ratio r between H_A and H_E is very small ($r = H_A/H_E \ll 1$), the onset of a surface spin–flop (SSF) phase was predicted using a continuum approximation [3, 4]. This phase is characterized by a canting near the surface and is stable for field values H greater than a critical value $H_{SSF} = \sqrt{H_E H_A + H_A^2} \approx H_{BSF}/\sqrt{2}$. Nearly a decade ago, the existence of such a surface spin–flop phase was criticized [5, 6] because a discrete, nonlinear map approach showed that the instability of the antiferromagnetic configuration at H_{SSF} simply leads to an interchange of the two sublattices [5, 6]. Subsequently Pokrovsky and Sinitsyn [7] showed that, for a semi-infinite film with $r \ll 1$, a quite similar result can also be obtained in the continuum approximation, provided that appropriate boundary conditions are assumed.

The case of a finite stack with an even number N of planes (but still $r \ll 1$) is quite different since, for $H_{SSF} < H < H_{BSF}$, the system tends to realize an inhomogeneous configuration with the magnetizations of both surfaces parallel to the field direction, and a domain wall is thus located in the centre of the stack. For $H > H_{BSF}$ the stable state of the finite film is a different inhomogeneous configuration, with the inner spins assuming nearly the bulk spin–flop configuration and the surface ones less deviated with respect to the field direction [6].

Fullerton *et al* [8] showed that the Fe/Cr(211) superlattice, obtained by the repetition of N ferromagnetic iron layers antiferromagnetically coupled through the Cr spacer, constitutes an excellent model system of a finite uniaxial antiferromagnetic film. Since then, a great number of papers [9–18] and [19][5] have been devoted to the study of the surface spin–flop phase transition. In fact, for sufficiently low thickness of the Fe layers, the system possesses a dominant uniaxial in-plane anisotropy along the Fe[0$\bar{1}$1] direction, with H_A of the same order of magnitude as H_E. For example, the Fe/Cr(211) superlattice [9] with thickness $t_{Fe} = 40$ Å and $t_{Cr} = 11$ Å had an anisotropy-to-exchange ratio $r = H_A/H_E \approx 1/4$, while for the system investigated in the present work and in [15], with $t_{Fe} = 14$ Å and $t_{Cr} = 11$ Å, one has $r \approx 1/10$. This is a major difference with respect to ordinary antiferromagnets, like MnF_2, where r is usually much smaller ($r \approx 1/100$). The consequence of an increased value of r in superlattices with respect to bulk antiferromagnets was investigated both experimentally [9] and theoretically [10, 11] in Fe/Cr(211) superlattices with $r \approx 1/4$, and was found to introduce a sequence of sudden jumps in the field dependence of the magnetization, in addition to the surface spin–flop jump occurring at H_{SSF}.

Recently, an accurate and systematic study of the phase diagram of a uniaxial antiferromagnetic film with an even number of planes was performed by Rößler and Bogdanov [19] using an efficient conjugate gradient minimization technique in the case of the external magnetic field applied precisely along the easy axis. For $r \ll 1$, they found that there is only a first-order transition from the collinear antiferromagnetic (AF) phase to a

[5] We note that for $N \geqslant 4$ the relationship between their notations and ours is the following: $H_E = 2J$ and $H_A = K$, so that the ratio $r = H_A/H_E \approx 0.1$ corresponds to $K/J \approx 0.2$ in the phase diagram of the film (e.g. reported in figure 6 of their preprint for the case $N = 12$).

symmetric, inhomogeneously flopped phase with the spin–flop (SF) located in the centre of the film. For $r \leqslant 1$, their calculations of the spin configuration confirmed previous theoretical findings [9, 11, 12]. In fact they found a series of canted, asymmetric phases (C_i), separated by first-order transition lines, between the AF and the SF phases [19]. Within these intermediate C phases, the ground state of the system evolves from a canted configuration with a flop localized near one of the surfaces (C_1) to other configurations ($C_2, C_3, \ldots$) where the flop moves into the centre, causing abrupt variations of the magnetization as the field intensity is increased [11, 19]. Finally, upon further increasing the anisotropy ($r > 1$), they found that only first-order transitions between collinear (antiferro-, ferri- and ferromagnetic) states are possible [19].

While the magnetic phase diagram of the finite AF film has been extensively investigated both theoretically and experimentally in the case of H applied parallel to the easy axis, no such studies are known for the case for which H is applied in-plane along an arbitrary direction with the easy axis. In the bulk case, the field-induced phase transition of a uniaxial antiferromagnet in the presence of a skew field forming an angle $\psi \neq 0°$ with the easy axis was theoretically studied by Rohrer and Thomas [20] using a mean-field approach and then by Fisher *et al* [21, 22]. Neglecting zero-point motion effects, they determined the equilibrium configurations as a function of the skew field, and found that the phase boundary between the AF and the bulk SF phase extends only to a maximum angle with respect to the easy axis, where it ends in critical points. More precisely, they predicted the first-order SF transition to become continuous (i.e., of second order) for ψ greater than a critical angle $\psi_{\max}(\text{bulk}) = \tan^{-1}[H_A/(2H_E - H_A)]$. This expression, first developed for a tetragonal system, was later found to be valid for an orthorhombic system, when ψ is restricted to a plane comprising the easy and intermediate axes [23].

The small values of $\psi_{\max}(\text{bulk})$ in ordinary bulk antiferromagnets (amounting to a few tenths of a degree) made the observation of the crossover from first to second order in the transition difficult. Early results on MnF_2 were, in this respect, only qualitative. More direct evidence of the crossover character of the transition was provided by Butera *et al* [24] by measuring the staggered magnetization of $MnCl_2{\cdot}4H_2O$. However, the existence and nature of a bicritical point was proven by measuring the critical magnetic scattering of a number of systems, notably $CuCl_2{\cdot}2H_2O$ [25], $CsMnBr_3{\cdot}2H_2O$ [26], and the above-mentioned $MnCl_2{\cdot}4H_2O$. On intuitive grounds, one might expect that in Fe/Cr(211) superlattices, a similar crossover effect in the order of the surface SF transition should be present and should be more easily observable owing to the higher value of the ratio $r = H_A/H_E$ ($r \approx 1/10$ or more) compared to ordinary bulk antiferromagnets like MnF_2, where $r \approx 1/100$.

The aim of the present paper is twofold: (i) to extend to the film (i.e., finite) case the theoretical study of the magnetic phase diagram of a uniaxial antiferromagnet in a skew field, and (ii) to provide experimental evidence that, in contrast to bulk antiferromagnets, in the case of the $[\text{Fe}(14\ \text{Å})/\text{Cr}(11\ \text{Å})]_{x20}$ superlattice, the crossover in the order of the surface SF transition with increasing skew field might be observed. Concerning the theoretical analysis, in section 2 we present two different approaches, the nonlinear map method and the Landau–Lifshitz–Gilbert micromagnetic simulation, for the ground-state and full hysteresis calculations, respectively. In section 3 experimental results, obtained by different techniques, are presented and discussed, both for H parallel to the easy axis ($\psi = 0°$) and for a skew field ($\psi \neq 0°$). Finally, conclusions are drawn in section 4.

2. Film model and theoretical framework

We consider a film made of an even number, N, of parallel ferromagnetic planes that are antiferromagnetically coupled one to each other by a nearest-neighbour exchange interaction

and subject to a uniaxial in-plane anisotropy. For thin magnetic layers, the magnetostatic dipolar interaction is known to confine the spins to the film plane, so that, at equilibrium, the spins are necessarily in-plane and the dipolar energy is zero. One can therefore characterize the spin configuration of the ith plane by only one parameter, namely the angle ϕ_i that the magnetization of the ith plane forms with the z axis (i.e., with the easy anisotropy axis) within the film plane xz. A magnetic field H is applied in the film plane along a direction that forms an angle ψ with z. At $T = 0$ K the energy density of the system takes the form

$$\begin{aligned} e &= E/(g\mu_B S N_\parallel) \\ &= \sum_{i=1}^{N} [H_E \cos(\phi_i - \phi_{i-1}) - H_A \cos^2 \phi_i - 2H_Z \cos\phi_i - 2H_X \sin\phi_i], \end{aligned} \tag{1}$$

where $N_\parallel$ denotes the number of spins within each film layer, and $H_Z = H\cos\psi$, and $H_X = H\sin\psi$.

The equilibrium spin configurations can be obtained from (1) by ϕ_i-derivation ($i = 1, \ldots, N$):

$$\begin{aligned} \frac{\partial e}{\partial \phi_i} = 0 = &-H_E \sin(\phi_i - \phi_{i-1})(1 - \delta_{1,i}) - H_E \sin(\phi_{i+1} - \phi_i)(1 - \delta_{N,i}) \\ &+ 2H_A \sin\phi_i \cos\phi_i + 2H_Z \sin\phi_i - 2H_X \cos\phi_i . \end{aligned} \tag{2}$$

In the present work, the ground state of the one-dimensional (1D) model (1) that approximates the film has been determined using two different theoretical methods, namely (i) an integration of the Landau–Lifshitz equation for the spin chain, introducing a damping coefficient in order to reach the magnetic ground state (see section 2.1), and (ii) a reformulation of equation (2), which provides the equilibrium conditions in terms of a nonlinear map with opportune boundary conditions at the film surfaces (see section 2.2). A comparative discussion of the two methods is made in section 2.3.

2.1. Spin configuration via integration of the Landau–Lifshitz–Gilbert equation

The Landau–Lifshitz–Gilbert (LLG) equation [27]

$$\frac{d\mathbf{M}}{dt} = -\gamma(\mathbf{M} \times \mathbf{H}_{eff}) + (\alpha_G/M_s)\left(\mathbf{M} \times \frac{d\mathbf{M}}{dt}\right) \tag{3}$$

describes the physical path of the magnetic moment $\mathbf{M}$ in a field $\mathbf{H}_{eff}$. Here γ and α_G are the gyromagnetic ratio of the free electron spin and the Gilbert damping coefficient respectively, M_s is the saturation magnetization, and $\mathbf{H}_{eff} = -(1/M_s)(\partial e/\partial \mathbf{M})$ is the local effective magnetic field. For thin magnetic layers, a large value of α_G is appropriate because the demagnetizing field confines the magnetic moment to the film plane, suppressing the gyromagnetic precession and leaving an in-plane rotation of the moment towards the direction of the local effective field. Thus, the integration of the LLG equation becomes a simple relaxation of the magnetic moment along the energy gradient. In the numerical calculations, we iteratively rotate spins that represent individual Fe layers by an amount proportional to the torque $\mathbf{M} \times (\mathbf{M} \times \mathbf{H}_{eff})$ at each instant. $\mathbf{H}_{eff}$ is then evaluated from the resulting configuration and applied to the next iteration. Upon reaching convergence, the stability of the equilibrium is tested by evaluating the eigenvalues of the stability matrix $M_{ij} = \partial^2 e/(\partial\phi_i \partial\phi_j)$ [10, 14]. All eigenvalues of the stability matrix must be positive for the state to be stable. In the event of an unstable equilibrium, the configuration $\{\phi_i\}$ is displaced by a random, small fraction along the eigenvector direction for which the eigenvalue is negative, and the relaxation process starts anew until the system reaches a stable *local* energy minimum.

2.2. Determination of the energy minima via the nonlinear map method

A different approach for the determination of the ground state of the magnetic system described by equation (1) was proposed some years ago [5, 6, 11]. It is based upon a reformulation of the equilibrium conditions (2) of the magnetic film model in terms of a discrete nonlinear map, where the film surfaces are introduced via opportune boundary conditions [28].

We start by introducing the new variable $s_i = \sin(\phi_i - \phi_{i-1})$, so that the conditions for an equilibrium spin configuration, equation (2), can be rewritten as a 2D nonlinear recursive map. For $1 < i < N$ one has

$$\begin{aligned} s_{i+1} &= s_i - (H_A/H_E)\sin(2\phi_i) - 2(H_Z/H_E)\sin\phi_i + 2(H_X/H_E)\cos\phi_i, \\ \phi_{i+1} &= \phi_i + \sin^{-1}(s_{i+1}). \end{aligned} \tag{4}$$

The trajectories in (ϕ, s) space are associated with equilibrium configurations, while the fixed points of the map correspond to uniform ground states of the infinite system and are second order (i.e., they satisfy the relation $(\phi_{n+2}, s_{n+2}) = (\phi_n, s_n)$) owing to its AF nature. We denote by (α, β) the ground-state configuration of the infinite system in the presence of a field of arbitrary direction. The angles α and β that the magnetizations of the two sublattices form with the easy axis can be determined by numerically solving the following problem of an extremum in two dimensions:

$$\begin{aligned} \partial e/\partial\alpha = 0 &= H_E\sin(\beta - \alpha) + (H_A/2)\sin(2\alpha) + H_Z\sin\alpha - H_X\cos\alpha, \\ \partial e/\partial\beta = 0 &= H_E\sin(\alpha - \beta) + (H_A/2)\sin(2\beta) + H_Z\sin\beta - H_X\cos\beta. \end{aligned} \tag{5}$$

From equation (5) it is readily found that the second-order fixed points of the map are $\mathrm{FP}_1 = (\beta, \sin(\beta - \alpha))$ and $\mathrm{FP}_2 = (\alpha, -\sin(\beta - \alpha))$. In order to study the map behaviour in the proximity of the fixed points, it is useful to perform a linear stability analysis of the doubly iterated map. It is worth noticing that energetically stable configurations (i.e., with a positive definite Hessian) are associated with topologically unstable (i.e., hyperbolic) trajectories in phase space. And, conversely, energetically unstable configurations are associated with topologically stable (i.e., elliptic) trajectories in phase space [28].

At this point, the presence of the two surface planes, signalled by the terms with the Kronecker δ in equation (2), is taken into account via opportune boundary conditions: i.e., we introduce two fictitious planes $i = 0$ and $N + 1$, so that we can assume the bulk equations, (4), to be valid even for the surface planes $i = 1$ and N, provided that the following equations are satisfied:

$$\begin{aligned} s_1 &= \sin(\phi_1 - \phi_0) = 0 \\ s_N &= \sin(\phi_{N+1} - \phi_N) = 0. \end{aligned} \tag{6}$$

In this way, among all trajectories obtained from the map equation (4), only those satisfying the boundary conditions (6) represent equilibrium configurations of the film with a finite number N of planes. In practice, the physical trajectories of the film must have two intersections with the $s = 0$ line, separated by exactly N steps of the recursive mapping [5, 6, 11].

Using this nonlinear map method, one is able to numerically determine all the stationary configurations of the film very rapidly and within machine precision. To find the ground state among the various calculated equilibrium configurations, it is necessary first to perform a linear stability analysis of the obtained solutions through the evaluation of the Hessian and then to compare the energies of the different metastable states in order to choose the lowest energy one.

2.3. Comparison of the two methods

By definition, the two theoretical methods described in sections 2.1 and 2.2 give the same results for the field evolution of the ground state from the AF to the SF phase. For the sake of

generality, a comparison between the two methods and a critical discussion of their respective advantages and drawbacks will now be presented.

The nonlinear map method allows one to determine all the equilibrium configurations of the film at zero temperature. Thus, comparing the energies of the various equilibrium configurations, one can easily determine the ground state. However, in the presence of two or more energetically equivalent ground states of different configurations, their knowledge is not enough to predict when a given equilibrium state is abandoned in favour of another equilibrium state as the intensity of the external field is varied. Such a process cannot be simulated in the framework of the nonlinear map method, whereas, in the approach based on the integration of the Landau–Lifshitz–Gilbert equation, the inclusion of the damping coefficient allows the system to evolve towards a stable local energy minimum. It should be noted that, in the framework of the latter method, the magnitude of perturbation applied during the stability test (i.e., the fractional displacement of the configuration $\{\phi_i\}$ in the event of an unstable equilibrium) may be crucial in determining which one of these states is eventually reached.

In this regard, we note that the problem of the determination of the actual state of the system may be nontrivial in the case of uniaxial anisotropy field and exchange field with comparable intensities, $r = H_A/H_E \approx 1$, as in Fe/Cr(211) superlattices for a suitable choice of the layer thicknesses [9]. In fact the metastability region turns out to be strongly amplified with respect to the case $r \ll 1$, and many metastable states with slightly different energies may be present, so that a tiny increment in the value of H may cause an abrupt change in the ground-state configuration [11, 16, 17]. Such a peculiar feature is usually signalled by a chaotic aspect of the nonlinear map in the (ϕ, s) phase space [6, 11]. In the extreme case of $r \gg 1$, fractal structures were predicted to appear both in the distribution of magnetic moments and in the energy spectrum [29].

As regards the [Fe(14 Å)/Cr(11 Å)]$_{x20}$ superlattice under study, in section 3 it will be shown that this system is characterized by a moderate value of the anisotropy ($r \approx 1/10$). As a consequence, the metastable state to which the system eventually relaxes in the micromagnetic calculations is not very sensitive to the magnitude of the perturbation applied during the stability test, so long as it is reasonably small. Thus, owing to the low value of r, the two theoretical methods were found to give quite similar results for the ground state of the Fe/Cr superlattice. (For the sake of precision, the results reported in figure 1 were obtained by the approach based upon the integration of the LLG equation, while those in figures 2, 6 and 7 were obtained via the nonlinear map method.)

Finally, it is worth observing that the theoretical results refer to the ground state, while experiments (as described in section 3) are performed at room temperature T_{amb}. The influence of a finite temperature on the spin–flop transition of a classical, simple cubic lattice, uniaxially anisotropic Heisenberg antiferromagnet was investigated some time ago [21]. Roughly speaking, comparing the $T = 0$ results with the experimental ones at T_{amb} is reasonable as long as $T_{amb} \lesssim T_b$, the bicritical point where the AF and SF ordered phases meet in the (H, T) phase diagram. For the square lattice, recent work [30] indicated that a very narrow disordered phase may intervene between the AF and the SF phase down to quite low temperatures, leading to the definition of a tetracritical point $T_t > T_b$. In both the $D = 3$ and 2 cases, the multicritical point in the (H, T) phase diagram was found to be a substantial fraction of T_N, the AF–paramagnetic transition temperature for $H = 0$. The Fe/Cr superlattice under study cannot be described by either of the two aforementioned models, since it is made of strongly ferromagnetic iron films, antiferromagnetically coupled through the chromium spacer. However, denoting by T_{mc} the multicritical point in the (H, T) phase diagram, one can expect $T_{mc} \lesssim T_N$ also in the superlattice case. In fact, on the basis of a mean-field theory estimate, T_N is expected to be

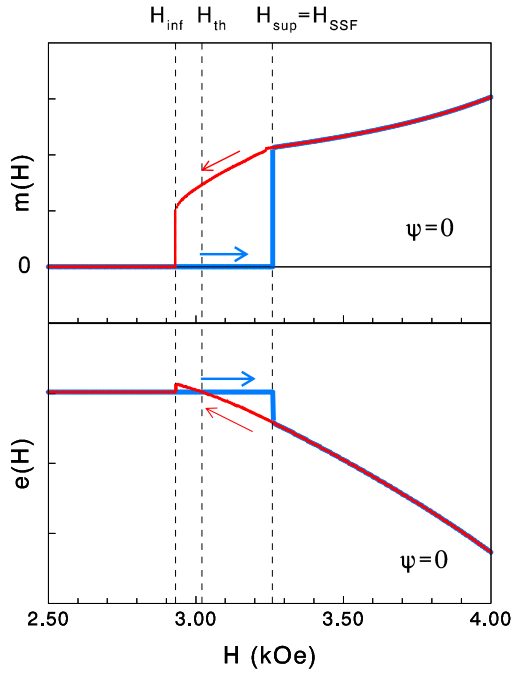

Figure 1. Calculated field dependence of the reduced magnetization, $m(H) = M/M_s$, and reduced energy $e(H)$, given by equation (1), of an antiferromagnetic film with $N = 20$ planes, for H in the neighbourhood of the surface spin–flop transition. The field is applied along the easy axis ($\psi = 0°$); the exchange field and the anisotropy field are, respectively, $H_E = 9.80$ kOe and $H_A = 0.98$ kOe. The thick (thin) line refers to increasing (decreasing) magnetic field. The field of thermodynamic equivalence between the energies of the collinear AF and the non-uniform SSF configuration is $H_{th} = 3.02$ kOe. The collinear AF state is stable for $H < H_{sup} = 3.26$ kOe; the non-uniform SSF state is stable for $H > H_{inf} = 2.93$ kOe; they have the same energy at H_{th}.

much greater than T_{amb} for the Fe/Cr superlattice, so that one can guess also the condition $T_{amb} \lesssim T_{mc}$ to be satisfied.

3. Experimental results

3.1. Sample characterization

The preparation and characterization of epitaxial Fe/Cr superlattices are similar to those described in [8]. The [Fe(14 Å)/Cr(11 Å)]$_{x20}$ superlattice was prepared [15] by dc magnetron sputtering onto a single-crystal MgO(110) substrate. To ensure epitaxy with the substrate, a 200 Å buffer layer of Cr was first deposited at 400 °C, then the superlattice was deposited at 100 °C and found to grow with a (211) orientation. Finally, a 100 Å capping layer of Cr was deposited to protect the sample. The epitaxy and the smoothness of the superlattice were checked by x-ray diffraction and found to have an interfacial roughness of ≈4 Å. Extensive magnetic characterizations were performed by means of magnetometry, as well as by magnetoresistance measurements. For Fe film thickness $t_{Fe} = 14$ Å, a strong, in-plane surface anisotropy $K_S = 0.06$ ergs cm^{-2} was found to develop along the [0$\bar{1}$1] direction, leading to a uniaxial in-plane anisotropy $K_U = 2K_S/t_{Fe} = 8.6 \times 10^5$ ergs cm^{-3} (compared to the bulk

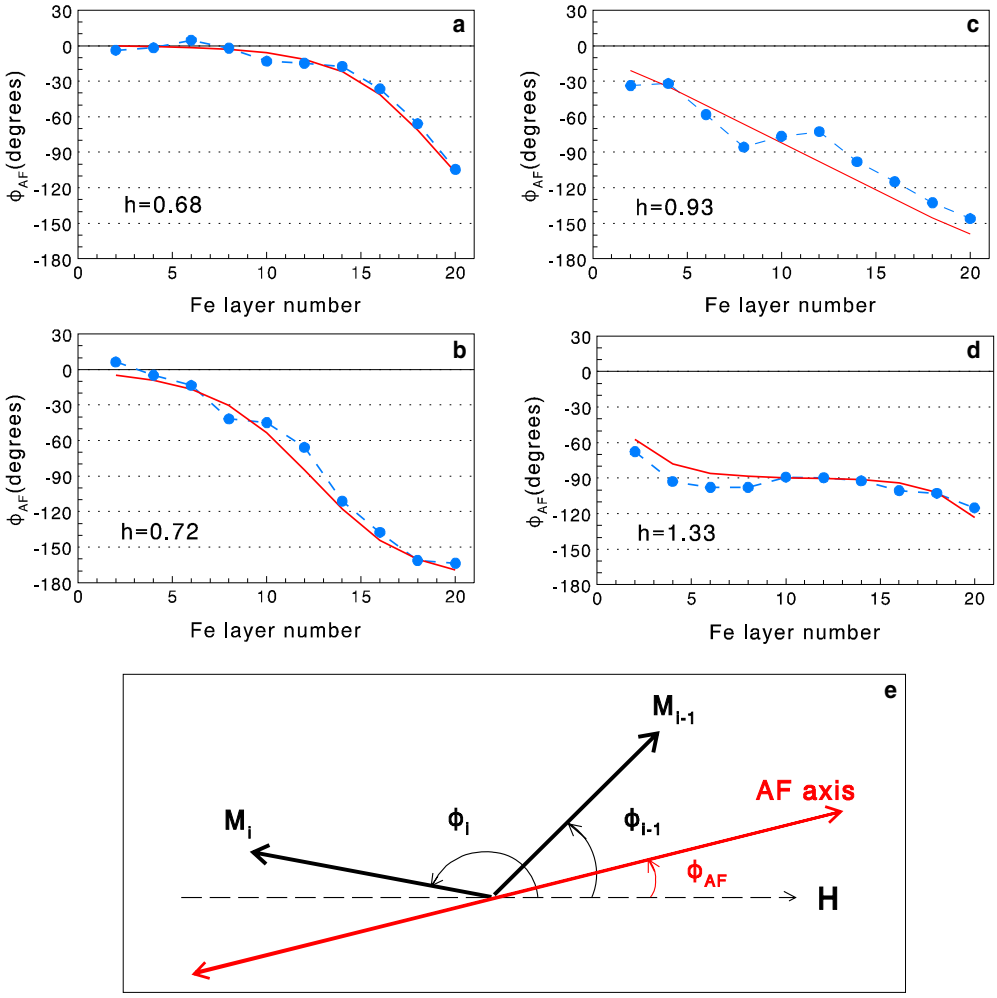

Figure 2. ((a)–(d)) Comparison between the calculated layer-by-layer configuration (solid lines) and the experimental ones (markers and dashed lines) deduced from polarized neutron reflectometry data in a [Fe(14 Å)/Cr(11 Å)]$_{x20}$ superlattice. The orientation ϕ_{AF} of the antiferromagnetic (AF) axis (i.e., the axis along which the magnetizations of two adjacent Fe layers are antiparallel) is plotted as a function of the Fe layer number for selected values of the reduced applied field ($h = H/H_{BSF}$); (e) schematic drawing showing that $\phi_{AF}(i) = \frac{1}{2}[\phi(i) + \phi(i-1)] - 90°$, where $\phi(i)$ is the angle formed by the magnetization $\mathbf{M}_i$ of the ith Fe layer with the field direction. The magnetic field is applied parallel to the easy axis ($\psi = 0°$).

crystalline anisotropy $K_1 = 4.7 \times 10^5$ ergs cm^{-3}). Using the value $M_s = 1740$ emu cm^{-3} of bulk Fe at $T = 0$ K, one obtains $H_A = 2K_U/M_s = 985.2$ Oe. The coupling between ferromagnetic layers was found to oscillate as a function of the thickness of the Cr interlayer. For $t_{Cr} = 11$ Å an AF exchange coupling with strength $J_{AF} = -1.194$ ergs cm^{-2} was estimated [8], leading to $H_E = 2|J_{AF}|/(t_{Fe}M_s) = 9802.9$ Oe.

For the [Fe(14 Å)/Cr(11 Å)]$_{x20}$ superlattice under study, previous SQUID measurements [15] of $M(H)$ versus H, applied in-plane along the easy axis of the sample, showed that M is zero for zero field. As H was increased, the instability of the AF phase was signalled by a steep increase of $M(H)$ at $H_{SSF} \approx 2.73$ kOe. In this study, M was measured using a vi-

brating sample magnetometer (VSM), in which the sample can be rotated so as that the in-plane magnetic field is applied at any skew angle ψ with respect to the easy axis.

3.2. Spin configuration for H parallel to the easy axis ($\psi = 0°$)

For H applied in-plane parallel to the easy axis ($\psi = 0°$), the calculation of the ground-state magnetization profiles shows that, in a limited field range near $H_{SSF} = \sqrt{H_E H_A + H_A^2}$, the system admits two stationary configurations: the AF state, with collinear and antiparallel layer magnetizations, and the surface spin–flop (SSF) state, with a non-uniform magnetization profile characterized by a Bloch wall that nucleates near one of the film surfaces. In figure 1 we plot, in the neighbourhood of H_{SSF}, the field dependence of the reduced magnetization, $m(H) = M/M_s = (1/N)\sum_{i=1}^{N} \cos\phi_i(H)$, and of the reduced energy $e(H)$, given by equation (1). Using for the calculations $H_E = 9.80$ kOe, $H_A = 0.98$ kOe, $N = 20$ and $\psi = 0°$, the field of thermodynamic equivalence between the AF and the SSF state is found to be $H_{th} = H(e_{AF} = e_{SSF}) = 3.02$ kOe, while the boundaries of the metastability region are given by the fields $H_{inf} = 2.93$ kOe and $H_{sup} = H_{SSF} = 3.26$ kOe. The AF state is the ground state for $H < H_{th}$ and is metastable for $H_{th} < H < H_{sup}$, while the SSF state is the ground state for $H > H_{th}$ and is metastable for $H_{inf} < H < H_{th}$. The calculated value of the bulk SF field is $H_{BSF} = \sqrt{2H_E H_A + H_A^2} = 4.50$ kOe.

In figures 2(a)–(d) the calculated ground-state magnetization profiles are compared with those obtained from polarized neutron reflectivity measurements, as published in [15], at different field values, ranging between 0 and 5.5 kOe. The fields $h = H/H_{BSF}$ were scaled with respect to the bulk SF field, where we set $H_{BSF} = 4.50$ kOe for the theoretical results and $H_{BSF} \approx 4.14$ kOe for the experimental ones. The orientation $\phi_{AF}(i)$ of the antiferromagnetic axis (i.e., the axis along which the magnetizations of two Fe adjacent layers are antiparallel) is plotted as a function of the Fe layer number for selected values of the applied field. Figure 2(e) illustrates that $\phi_{AF}(i) = \frac{1}{2}[\phi(i) + \phi(i-1)] - 90°$, where $\phi(i)$ is the angle formed by the magnetization $\mathbf{M}_i$ of the ith Fe layer with the field direction. As the measured spectrum extends only as far as the half-order AF Bragg peak, which is determined by the antiparallel components of the magnetizations, the orientation $\phi_{AF}(i)$ of the AF axis is obtained with more accuracy from the experiments than that of the individual layer orientations, for which the estimated error is up to 20° [15]. This representation clearly depicts the position and extent of the domain wall for the different fields and shows that agreement between theory and experiment is fairly good.

From figures 2(a)–(d) one sees that the basic features of the SSF transition in this film, characterized by a low value of $r \approx 1/10$, are the following: (i) for $H > H_{SSF}$ the deviations from the uniform AF spin configuration originate just at the surface layer whose magnetization is antiparallel to the field; (ii) with increasing H, the surface-nucleated domain wall is pushed gradually into the middle of the film; (iii) for $H > H_{BSF}$ a symmetric spin configuration is achieved, similar to the bulk SF one in the middle planes (while the spins at the surfaces, owing to the cuts of the exchange bonds, are less deviated from the field direction with respect to the bulk ones). Although not directly obvious from figure 2, the discommensuration [12] at the centre of the surface-nucleated domain wall, effectively dividing the AF order into two antiphase domains, which was strongly evidenced by the neutron data [15], is also reproduced by the calculations.

Note that no abrupt variations of the magnetization, except the one at H_{SSF}, are found as the field intensity is increased; see figure 1: i.e., additional first-order transitions between C phases, intermediate between the AF and the SSF one [11, 19], are not allowed by the low value of $r = H_A/H_E$ in this system.

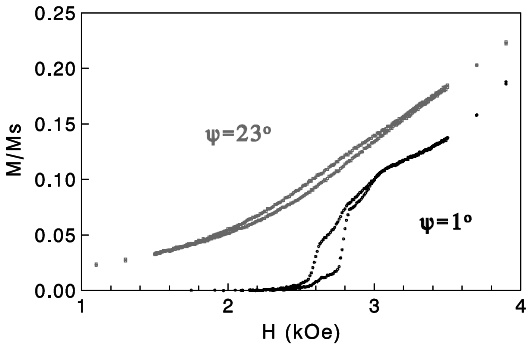

Figure 3. Experimental VSM data for the magnetization $M(H)$ of a [Fe(14 Å)/Cr(11 Å)]$_{x20}$ superlattice versus H, applied along a direction which forms a skew angle ψ with the easy in-plane axis. The two different curves refer to $\psi = 1°$ and 23°, respectively.

3.3. Spin configuration for H applied along an arbitrary direction ($\psi \neq 0°$)

For a field applied in-plane along an arbitrary direction forming a skew angle $\psi \neq 0°$ with the easy axis (i.e., both H_X and H_Z are non-zero), one has that $M(H) = 0$ for $H = 0$. For $0° < \psi < 5°$, $M(H)$ increases slowly with increasing H, since for $\psi \neq 0°$ the magnetizations of the two sublattices are no longer compensated. Upon further increasing H, a finite jump, signalling the onset of a first-order phase transition, was observed for a ψ-dependent field value. The measurements were performed both upon increasing and decreasing H, and showed a marked hysteresis for such small ψ values; see figure 3. The magnetic susceptibility $\chi(H) = \mathrm{d}M/\mathrm{d}H$, obtained by numerically deriving the measured magnetization with respect to H, showed sharp peaks corresponding to the jumps in $M(H)$; see figure 4, top. The full width at half maximum (FWHM; see figure 5, top) of the measured susceptibility peak was found to be constant and very small (essentially determined by the instrumental resolution), signalling that for such small angle values ($0° < \psi < 5°$) the SSF transition is of first order.

As ψ was gradually increased above 5°, $M(H)$ became smoother (see figure 3), and the peak in $\chi(H)$ (see figure 4, bottom) decreased in intensity, while the FWHM dramatically increased on passing from 5° to 23°, as shown in figure 5, top. The latter feature strongly suggests that a crossover of the surface phase transition from first order to second order might take place for $\psi \geqslant 5°$.

In the light of this interpretation, it is however necessary to justify the persistence—up to the highest investigated value of ψ (23°)—of a small hysteresis loop; see figure 5, bottom, where the measured dependence of the peak position of the magnetic susceptibility $\chi(H)$ is shown as a function of the skew angle ψ, both for increasing (full circles) and decreasing (open circles) magnetic field.

To this aim, we observe that the coexistence of first- and second-order transition features was recently observed [31] in single-crystal $La_{0.73}Ca_{0.27}MnO_3$ perovskites exhibiting colossal magnetoresistance. The magnetization isotherms displayed a metamagnetic structure linked with a first-order transition, while field- and temperature-dependent ac susceptibility data presented a crossover line characteristic of a continuous transition [31].

In our case of a finite AF Fe/Cr(211) film, a similar effect, i.e., the coexistence of first- and second-order transition features, might be attributed to a distribution of values of the interlayer exchange, as well as of the anisotropy of the different layers in the stack, due to the presence of thickness fluctuations. In determining the observed small hysteresis loop, one also cannot rule

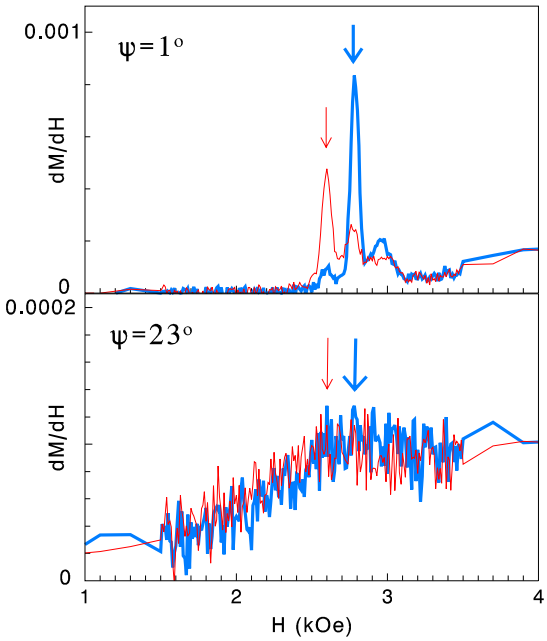

Figure 4. Experimental data for the magnetic susceptibility $\chi(H) = \mathrm{d}M/\mathrm{d}H$ of a [Fe(14 Å)/Cr(11 Å)]$_{x20}$ superlattice, obtained by numerically deriving the VSM data in figure 3, both for increasing field (thick line) and decreasing field (thin line). Top diagram: $\psi = 1°$; bottom diagram: $\psi = 23°$. In each diagram, the arrow at the lower (higher) field denotes the peak position for decreasing (increasing) H.

out the role of defects (pinning centres) which inhibit the lateral motion of domains during the magnetization reversal process.

In the following we will test if the experimental data can be explained in terms of a crossover from first- to second-order critical behaviour by performing a theoretical calculation of the magnetization profile $\{\phi_i; i = 1, \ldots, N\}$ for different values of H and $\psi \neq 0°$, using either of the two methods described in section 2. In the present case where $r \ll 1$, the map portrait is not chaotic and the two different methods give similar results. From the calculated spin configuration, one obtains $m(H) = M/M_s = (1/N)\sum_{i=1}^{N} \cos\phi_i$, $\chi(H) = \mathrm{d}M/\mathrm{d}H$ and $e(H)$, given by equation (1).

We find that for $0° < \psi < 4.75°$ the system admits two stationary configurations: a nearly AF state and an SSF state. The first one is stable only for $H < H_{sup}$ while the second one is stable only for $H > H_{inf}$. By H_{th} we denote the field of thermodynamic equivalence at which the two states take the same energy. As ψ increases, the width of the metastability region gradually reduces until, for $\psi > 4.75°$, only one equilibrium configuration is found.

In figure 6 the calculated susceptibility $\chi(H)$ is shown for different values of the skew angle ψ. For $\psi \leqslant 3°$, the peak in $\chi(H)$ is a Dirac delta function, so the peak position is indicated by a vertical line. For $\psi \geqslant 5°$ the peak has a finite width and a finite height. As ψ increases, the peak broadens and its height decreases. For clarity's sake, the peak position reported in figure 6 for $\psi \leqslant 3°$ corresponds to the calculated field of thermodynamic equivalence H_{th} between the energies of the AF-like configuration and the non-uniform SSF configuration. It is just the position of this peak that is reported versus ψ in figure 7 as the full-circle diagram; the other two diagrams plotted for $\psi \leqslant 4.75°$ represent the calculated field values H_{inf} (open squares) and H_{sup} (open triangles) versus ψ.

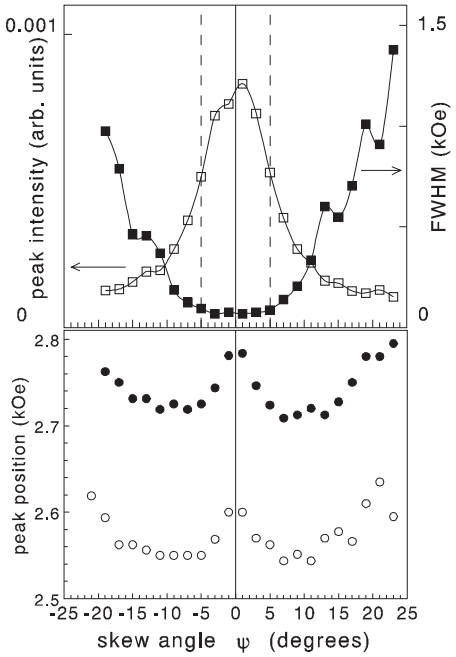

Figure 5. Top diagram: experimental peak intensity (open squares) and FWHM (full squares) of the magnetic susceptibility $\chi(H)$ of a [Fe(14 Å)/Cr(11 Å)]$_{x20}$ superlattice versus the skew angle ψ formed by the applied magnetic field with the easy in-plane axis. The lines are guides to the eye. A dramatic increase in the FWHM is observed for $|\psi| > 5°$. Bottom diagram: experimental peak position of $\chi(H)$ versus ψ, both for increasing (full circles) and decreasing (open circles) field intensity.

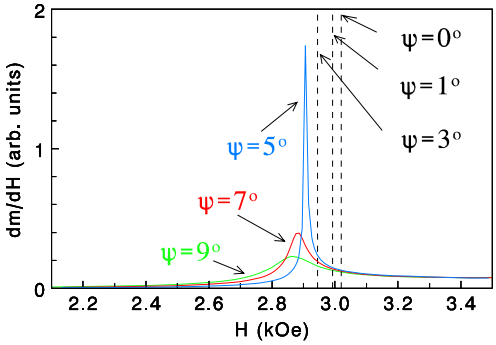

Figure 6. Calculated $\chi(H) = \mathrm{d}M/\mathrm{d}H$ of an AF film with $N = 20$ and $H_{\mathrm{E}} = 9.80$ kOe, $H_{\mathrm{A}} = 0.98$ kOe versus H applied in-plane along an arbitrary direction. The different curves refer to different values of the skew angle ψ formed by the external magnetic field with the easy axis. For $\psi \leqslant 3°$, the position of the reported peak of $\chi(H)$ is indicated by a vertical dashed line and corresponds to the field of thermodynamic equivalence H_{th} between the energies of the AF-like and the non-uniform SSF configuration.

In the phase diagram of figure 7 one clearly observes that, upon increasing ψ, the width of the metastability region gradually shrinks until, for ψ greater than a critical value $\psi_{\mathrm{max}}(\mathrm{film}) = 4.75°$, the film admits only one equilibrium state. Thus, for $\psi \geqslant \psi_{\mathrm{max}}(\mathrm{film})$ we expect the SSF transition to become continuous. The calculated value of $\psi_{\mathrm{max}}(\mathrm{film}) = 4.75°$

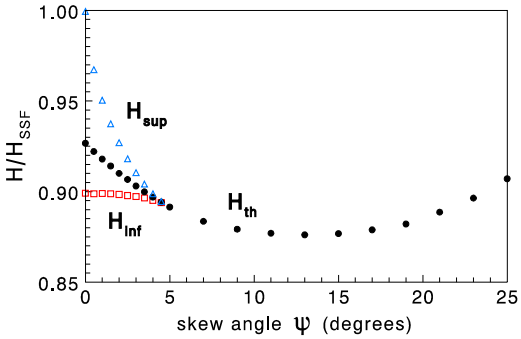

Figure 7. Calculated phase diagram of an AF film with $N = 20$ and $H_E = 9.80$ kOe, $H_A = 0.98$ kOe. The peak positions of $\chi(H) = dM/dH$, scaled with respect to H_{SSF}, are reported versus the skew angle ψ formed by the external magnetic field with the easy axis. For $\psi > 4.75°$ the SSF transition is predicted to become continuous. The calculated field of thermodynamic equivalence H_{th} is reported versus ψ as the full-circle diagram; the other two diagrams plotted for $\psi \leqslant 4.75°$ represent the calculated field values H_{inf} (open squares) and H_{sup} (open triangles).

turns out to be in remarkable agreement with the value ≈5° estimated from the experimental results on the basis of the strong increase observed in the FWHM of $\chi(H)$. This fact provides support for the hypothesis of a crossover from first- to second-order critical behaviour for the SSF transition in a skew field.

The calculated value of $\psi_{max}(\text{film}) = 4.75°$ should also be compared with its bulk counterpart. In the bulk case, the field-induced phase transition of a uniaxial antiferromagnet in the presence of a skew field forming an angle ψ with the easy axis was theoretically studied by Rohrer and Thomas [20]. They predicted the first-order bulk SF transition to become continuous for $\psi \geqslant \psi_{max}(\text{bulk}) = \tan^{-1}[H_A/(2H_E - H_A)]$. However, in MnF_2, where $r \approx 1/100$, the critical angle turns out to be as small as ≈0.4°. In the case of the Fe/Cr superlattice under study, the ratio r is nearly an order of magnitude higher than in MnF_2, so that an appreciable critical angle $\psi_{max}(\text{bulk}) \approx 3°$ is estimated. The calculated value of $\psi_{max}(\text{film}) = 4.75°$ is nearly twice the bulk value. This can be qualitatively understood considering that, for not too high values of r, in the bulk the critical angle is essentially determined by the ratio $H_A/(2H_E)$, while in the film the effective exchange field at the surface is halved with respect to the bulk.

4. Discussion

In this work we have investigated the transition, induced by a magnetic field H with arbitrary direction, between the antiferromagnetic phase and the surface spin–flop phase of an epitaxial Fe/Cr(211) superlattice with $t_{Fe} = 14$ Å, $t_{Cr} = 11$ Å and $N = 20$ repetitions. The system is characterized by a rather small value ($r \approx 1/10$) of the ratio $r = H_A/H_E$ between the uniaxial anisotropy field H_A and the exchange field H_E, yet much greater than the value ($r \approx 1/100$) pertinent to usual bulk antiferromagnets like MnF_2 and Cr_2O_3.

For an external field applied parallel to the easy in-plane axis ($\psi = 0°$), the layer-by-layer spin configurations measured by polarized neutron reflectometry were found to be in remarkable agreement with theoretical calculations, performed in the framework of a mean-field 1D model of the superlattice stack.

For a field applied in-plane along an arbitrary direction forming a skew angle $\psi \neq 0°$ with the easy axis, the superlattice magnetization $M(H)$ was measured using magnetometry. The

phase diagram of the film was calculated in order to check the possibility of a crossover of the surface phase transition from first to second order to take place for $\psi_{\max}(\text{film})$, similarly to what was predicted decades ago by Rohrer and Thomas [20] for an AF bulk system in a skew field. Indeed we calculated $\psi_{\max}(\text{film}) \approx 4.75°$, to be compared with the experimental value, $\psi \approx 5°$, at which the jump in $M(H)$ starts smoothening and the FWHM of the measured magnetic susceptibility displays a dramatic increase with increasing ψ. Owing to the cut of exchange bonds at the film surfaces, the calculated value of $\psi_{\max}(\text{film})$ turns out to be nearly twice its bulk counterpart, $\psi_{\max}(\text{bulk}) \approx 3°$ [20]. The latter value is much higher than the ones predicted for ordinary bulk antiferromagnets (e.g., $\psi_{\max}(\text{bulk}) \approx 0.4°$ for MnF_2 and $\approx 0.015°$ for Cr_2O_3) [20].

From the comparison between our experimental and theoretical results we conclude that a crossover between first- and second-order critical behaviour is easier to be observed by magnetization measurements in Fe/Cr superlattices, thanks to the much higher value of the ratio $r = H_A/H_E$ between the anisotropy and the exchange fields in such an artificially grown system with respect to ordinary bulk antiferromagnets.

The interpretation of the experimental data proposed above needs, however, further investigation to be conclusive. In particular, a quantification of the magnetic domain structure in the presence of a structurally rough interface is required. While our previously published [15] polarized neutron reflectometry data proved unambiguously that only one type of domain is present in Fe/Cr(211) superlattices with an interfacial roughness of ≈ 4 Å for zero field, such clear-cut evidence is lacking in the case of a non-zero field, applied in plane along an arbitrary direction. In conclusion, while we do not claim a quantitative accuracy for our theoretical results, nevertheless we believe that the main features of the spin–flop transition in the Fe/Cr superlattice have been captured by our 'ideal' model (i.e., characterized by structurally smooth and uniformly magnetized layers).

Acknowledgments

Financial support from the Italian Ministry for University and Research is acknowledged. This work was performed in the framework of the joint CNR-MIUR programme (legge 16/10/2000, Fondo FISR) and of the COFIN Project on Magnetic Multilayers. The work at Argonne National Laboratory was supported by the US Department of Energy, Office of Science, under contract W-31-109-ENG-38.

References

[1] Néel L 1936 *Ann. Phys. Fr.* **5** 232
[2] Anderson F B and Callen H B 1964 *Phys. Rev.* **136** A1068
[3] Mills D L 1968 *Phys. Rev. Lett.* **20** 18
Saslow W and Mills D L 1968 *Phys. Rev.* **171** 488
[4] Keffer F and Chow H 1973 *Phys. Rev. Lett.* **31** 1061
[5] Trallori L, Politi P, Rettori A, Pini M G and Villain J 1994 *Phys. Rev. Lett.* **72** 1925
[6] Trallori L, Pini M G, Rettori A, Macciò M and Politi P 1996 *Int. J. Mod. Phys.* B **10** 1935
[7] Pokrovsky V L and Sinitsyn N A 2002 private communication
[8] Fullerton E E, Conover M J, Mattson J E, Sowers C H and Bader S D 1993 *Phys. Rev.* B **48** 15755
[9] Wang R W, Mills D L, Fullerton E E, Mattson J E and Bader S D 1994 *Phys. Rev. Lett.* **72** 920
[10] Wang R W and Mills D L 1994 *Phys. Rev.* B **50** 3931
[11] Trallori L, Politi P, Rettori A, Pini M G and Villain J 1995 *J. Phys.: Condens. Matter* **7** L451
[12] Micheletti C, Griffiths R B and Yeomans J M 1997 *J. Phys. A: Math. Gen.* **30** L233
Micheletti C, Griffiths R B and Yeomans J M 1999 *Phys. Rev.* B **59** 6239
[13] Trallori L 1998 *Phys. Rev.* B **57** 5923

[14] Dantas A L and Carrico A S 1999 *Phys. Rev.* B **59** 1223
[15] te Velthuis S G E, Jiang J S, Bader S D and Felcher G P 2002 *Phys. Rev. Lett.* **89** 127203
[16] Bogdanov A N and Rößler U K 2003 *Phys. Rev.* B **68** 012407
[17] Rößler U K and Bogdanov A N 2004 *Phys. Rev.* B **69** 094405
[18] Rößler U K and Bogdanov A N 2004 *Phys. Rev.* B **69** 184420
[19] Rößler U K and Bogdanov A N 2004 *Phys. Status Solidi* C **1** 3297
[20] Rohrer H and Thomas H 1969 *J. Appl. Phys.* **40** 1025
[21] Fisher M E and Nelson D R 1974 *Phys. Rev. Lett.* **32** 1350
[22] Kosterlitz J M, Nelson D R and Fisher M E 1976 *Phys. Rev.* B **13** 412
[23] Blazey K W, Rohrer H and Webster R 1977 *Phys. Rev.* B **4** 2287
[24] Butera R A, Corliss L M, Hastings J M, Thomas R and Mukamel D 1981 *Phys. Rev.* B **24** 1244
[25] Lynn J W, Heller P and Lurie N A 1977 *Phys. Rev.* B **16** 5032
[26] Bastee J A J, Frikkee E and de Jonge W J M 1980 *Phys. Rev.* B **22** 1429
[27] Landau L D and Lifshitz E 1935 *Phys. Z. Sowietunion* **8** 153–69
[28] Pandit R and Wortis M 1982 *Phys. Rev.* B **25** 3226
[29] Kürten K E and Kusmartsev F V 2005 *Phys. Rev.* B **72** 014433
[30] Holtschneider H, Selke W and Leidl R 2005 *Phys. Rev.* B **72** 064443
[31] Li W, Kunkel H P, Zhou X Z, Williams G, Mukovskii Y and Shulyatev D 2004 *J. Phys.: Condens. Matter* **16** L109